Cell, Vol. 113, 249–260, April 18, 2003, Copyright ©2003 by Cell Press

Desmoglein 4 in Hair Follicle Differentiation and Epidermal Adhesion: Evidence from Inherited Hypotrichosis and Acquired Pemphigus Vulgaris

Ana Kljuic,[1] Hisham Bazzi,[1] John P. Sundberg,[4] Amalia Martinez-Mir,[2] Ryan O'Shaughnessy,[2] My G. Mahoney,[5] Moise Levy,[6] Xavier Montagutelli,[7] Wasim Ahmad,[2,12] Vincent M. Aita,[2] Derek Gordon,[9] Jouni Uitto,[5] David Whiting,[8] Jurg Ott,[9] Stuart Fischer,[3] T. Conrad Gilliam,[1,3] Colin A.B. Jahoda,[10] Rebecca J. Morris,[2] Andrei A. Panteleyev,[2] Vu Thuong Nguyen,[11] and Angela M. Christiano[1,2,*]

[1]Department of Genetics and Development
[2]Department of Dermatology
[3]Columbia Genome Center
Columbia University
New York, New York 10032
[4]The Jackson Laboratory
Bar Harbor, Maine 04609
[5]Department of Dermatology and Cutaneous Biology
Jefferson Medical College
Philadelphia, Pennsylvania 19107
[6]Baylor College of Medicine
Houston, Texas 77030
[7]Unite de Genetique des Mammiferes
Institut Pasteur 75724
Paris, France
[8]Dallas Associated Dermatologists
Dallas, Texas 75246
[9]Laboratory for Statistical Genetics
Rockefeller University
New York, New York 10021
[10]Durham University DH1 3LE
Durham, United Kingdom
[11]Department of Dermatology
University of California, Davis
Davis, California 95817

Summary

Cell adhesion and communication are interdependent aspects of cell behavior that are critical for morphogenesis and tissue architecture. In the skin, epidermal adhesion is mediated in part by specialized cell-cell junctions known as desmosomes, which are characterized by the presence of desmosomal cadherins, known as desmogleins and desmocollins. We identified a cadherin family member, desmoglein 4, which is expressed in the suprabasal epidermis and hair follicle. The essential role of desmoglein 4 in skin was established by identifying mutations in families with inherited hypotrichosis, as well as in the *lanceolate hair* mouse. We also show that DSG4 is an autoantigen in pemphigus vulgaris. Characterization of the phenotype of naturally occurring mutant mice revealed disruption of desmosomal adhesion and perturbations in keratinocyte behavior. We provide evidence that desmoglein 4 is a key mediator of keratinocyte cell adhesion in the hair follicle, where it coordinates the transition from proliferation to differentiation.

*Correspondence: amc65@columbia.edu
[12]Present address: Department of Biological Sciences, Quaid-i-Azam University, Islamabad, Pakistan.

Introduction

The hair follicle (HF) is among the few mammalian organs which periodically reverts to a morphogenic program of cellular events as a part of its normal cycle of growth (anagen), involution (catagen), and quiescence (telogen) (Fuchs et al., 2001; Hardy, 1992). The HF develops as the result of a series of reciprocal epithelial-mesenchymal signals between the dermal papilla (DP) and the overlying epithelium during morphogenesis. It is the transmission of morphogenic signals via elaborate networks of cell contacts during development that transforms simple sheets of epithelial cells into complex three-dimensional structures, such as the HF (Fuchs et al., 2001; Jamora and Fuchs, 2002). The cellular rearrangements that occur with each adult mouse hair cycle are no less dynamic and well-orchestrated, given that the entire population of hair matrix keratinocytes is reduplicated in approximately 13 hr (Bullough and Laurence, 1958; Van Scott et al., 1963). Keratinocytes in the lowermost HF are multipotent and proliferate rapidly until they pass through a zone parallel to the widest part of the DP, known as the "critical region" or the line of Auber (Auber, 1952) above which mitosis ceases, differentiation begins, and the gradual elongation of cells takes place as they ascend and form the concentric layers of the HF.

The determination of keratinocyte cell fate in the lower HF is governed by morphogens including bone morphogenic proteins (BMPs) and sonic hedgehog (Shh), membrane bound signaling molecules such as Notch and Delta, and secreted growth factors such as Wnts and FGFs, whose expression is active during HF morphogenesis and is reprised in each adult hair cycle (Fuchs et al., 2001; Jamora and Fuchs, 2002). The network of cell-cell junctions that provides the infrastructure for transmission of these signals is critical for imparting information to the proliferating keratinocytes to direct them down one of several specific differentiation pathways (Orwin, 1979). To meet the demand for sophisticated communication and signaling events orchestrated by cell-cell adhesion, the number of desmosomes more than doubles during differentiation (Orwin, 1979), such that in a mature HF, up to 90% of the cell surfaces of the individual keratinocyte layers within the inner root sheath (IRS) are occupied by desmosomes (Roth and Helwig, 1964). The line of Auber represents an information portal through which multipotent keratinocytes must quickly pass, receiving instructions that determine their destiny as they enter, and executing highly intricate programs of differentiation upon their exit.

Intercellular junctions are critical for orchestrating the molecular events during HF induction and cycling, which require synchronization of the transition from proliferation to differentiation (Jamora and Fuchs, 2002). Desmosomes are elaborate multiprotein complexes that link cadherin partners to the intermediate filament (IF) net-

work via plakin and armadillo family members (Fuchs et al., 2001; Green and Gaudry, 2000). In mouse and human, three desmoglein (*DSG1,2,3*) and three desmocollin (*DSC1,2,3*) genes have been described previously. DSG1, DSC1, DSG3, and DSC3 are predominantly expressed in stratifying squamous epithelia such as the epidermis, whereas DSG2 and DSC2 are present in simple epithelia and nonepithelial tissues as well. In the epidermis, DSG1 and DSC1 are expressed in the suprabasal layers of the epidermis, while DSG3 and DSC3 are present in the basal layer (Garrod et al., 2002; Green and Gaudry, 2000). DSG1 and DSG3 also serve as autoantigens in the acquired bullous dermatoses, pemphigus foliaceus and pemphigus vulgaris (PV), respectively, which are characterized by loss of cell-cell adhesion in the epidermis (Green and Gaudry, 2000; McMillan and Shimizu, 2001). Desmosomes impart structural integrity to tissues undergoing mechanical stress, and recent evidence suggests that they may also regulate the availability of signaling molecules and transduce signals that dictate the state of the cytoskeleton and activate downstream genetic programs (Fuchs et al., 2001; Green and Gaudry, 2000).

The critical role of the desmosomal proteins in epithelial integrity has been illustrated by targeted ablation of the corresponding genes in mice, as well as their disruption in human diseases. The phenotypes that arise in these mice range from embryonic lethal, such as *Dsg2*, desmoplakin (*Dsp)*, and plakoglobin (*Pg)* (Eshkind et al., 2002; Jamora and Fuchs, 2002), to relatively mild, as in *Dsc1* null animals (Chidgey et al., 2001), or *Dsg3* null animals which are allelic to the spontaneous, cyclical *balding* mouse (Koch et al., 1997; Montagutelli et al., 1997; Pulkkinen et al., 2002). Nonlethal mutations in the genes encoding desmosomal proteins have also been identified in humans (McMillan and Shimizu, 2001). With the exception of *DSG1*, these disorders are unified by profound abnormalities in the HF. For example, mutations in *DSP* and *PG* underlie Naxos disease, characterized by woolly, sparse hair, keratoderma, and cardiomyopathy (McKoy et al., 2000; Norgett et al., 2000); plakophilin I (*PKP1)* mutations cause ectodermal dysplasia with sparse hair and skin fragility (McGrath et al., 1997); and keratodermas result from mutations in either *DSG1* or *DSP* (Armstrong et al., 1999; Hunt et al., 2001; Kljuic et al., in press). While these models have provided significant insights into the role of intercellular adhesion proteins in epidermal cytoarchitecture in either mouse or human, examples have not yet emerged of desmosomal proteins for which direct parallels between a human genetic disease, an acquired autoimmune disease, and corresponding mouse models can be drawn.

It is puzzling that despite the preponderance of desmosomes in the inner layers of the hair shaft, and their critical role in intercellular adhesion, none of the known desmosomal cadherin genes are highly expressed in this region (Koch et al., 1997; Kurzen et al., 1998). Using a classical genetic approach, we discovered a fourth member of the desmosomal cadherin gene superfamily, desmoglein 4 (*DSG4*), which is expressed in both the suprabasal epidermis and extensively throughout the matrix, precortex, and IRS of the HF. We identified causative mutations in desmoglein 4 underlying both an inherited form of human hypotrichosis, and the *lanceolate* mouse models. Further, we show that DSG4 serves as an autoantigen in the sera of patients with PV. Characterization of the phenotype of mutant mouse epidermis revealed a hyperproliferative phenotype, including suprabasal expression of β1 integrin and ectopically proliferating cells. In the lower HF, we discovered a premature switch from proliferation to differentiation, as well as perturbations in the onset of hair shaft differentiation programs. Our findings establish a central role for desmoglein 4 in epidermal cell adhesion, and in coordinating the transition from proliferation to differentiation in HF keratinocytes.

Results

Localized Hypotrichosis Is Linked to Chromosome 18

Two consanguineous Pakistani pedigrees with localized autosomal recessive hypotrichosis (LAH) were collected (Figures 1A and 1B) in which affected members display hypotrichosis (Figures 2A–2D) restricted to the scalp, chest, arms, and legs. Facial hair, including the eyebrows and beard, is less dense, and axillary, pubic hair, and eyelashes are spared. Overall, the patients' skin is normal with the exception of patches of scalp where small papules are visible that are likely a consequence of ingrown hairs. Histological analysis of scalp skin reveals abnormal HF and hair shafts (Figures 2I and 2K) that are thin and atrophic and often appear coiled up within the skin due to their inability to penetrate the epidermis (Figure 2K). Another striking defect is a marked swelling of the precortical region resulting in the formation of a bulbous "bleb" within the base of the hair shaft (Figure 2I).

To identify the gene underlying the LAH phenotype, we followed a classical linkage analysis approach. Prior to embarking on a genome-wide scan, we performed cosegregation and homozygosity analysis with microsatellite markers corresponding to candidate genes involved in related phenotypes. These included the desmosomal cadherin gene cluster on 18q12, the hairless gene on 8p21, the nude gene on 17q11, and the keratin clusters on chromosomes 12 and 17. Linkage was excluded for all regions, with the exception of the desmosomal cadherin gene cluster on chromosome 18. A maximum two-point LOD score (Z_{max}) of 4.63 was obtained for marker D18S866 ($\theta = 0$), combining the LOD score values from the two pedigrees (Figure 1C). Multipoint analysis supported linkage to this region, with maximum LOD scores exceeding 5.0 throughout the interval D18S1149-D18S1135 (Figure 1D).

A key recombination event in individual IV-10 from pedigree LAH-1 (Figure 1A) placed the LAH locus telomeric to D18S1149. Haplotype analysis using chromosome 18 markers (Figures 1A and 1B) revealed that affected individuals were homozygous for markers in D18S1108–D18S1135, and shared an identical genotype for D18S36. According to the physical map from the Human Genome Project Working Draft (April 2002 release), D18S36 lies 0.5 Mb centromeric to the desmosomal cadherin gene cluster (Buxton et al., 1993). All exons and splice sites from the six genes were sequenced in affected members from both families; however, no mutations were identified.

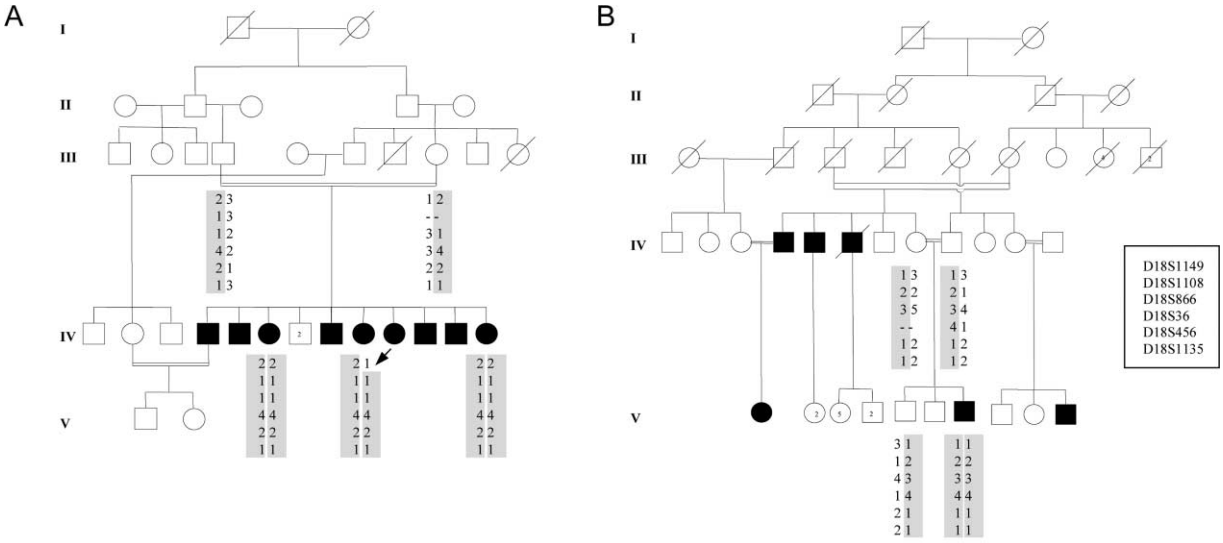

C

		LOD score at θ =						
Marker	**cM**	**0.00**	**0.01**	**0.05**	**0.10**	**0.20**	**0.30**	**0.40**
D18S1149	49.55	-∞	3.11	**3.36**	3.08	2.20	1.24	0.43
D18S1108	51.21	2.15	2.09	1.88	1.62	1.14	0.70	0.29
D18S866	52.03	**4.63**	4.53	4.10	3.57	2.51	1.49	0.58
D18S36	58.45	2.51	2.45	2.21	1.91	1.33	0.77	0.27
D18S456	61.73	**3.30**	3.22	2.89	2.48	1.68	0.94	0.34
D18S1135	61.73	2.22	2.16	1.95	1.69	1.15	0.66	0.25

D

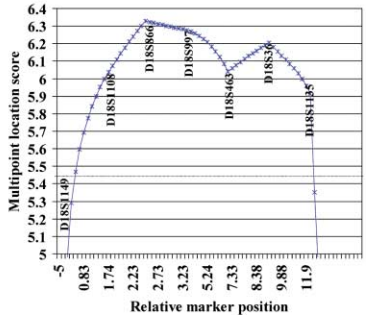

Figure 1. Linkage Analysis in LAH Pedigrees

(A and B) Haplotypes for chromosome 18 markers are shown for representative individuals in pedigrees LAH-1 (A) and LAH-2 (B). The key recombination event in IV-10 between markers D18S1149 and D18S1108 is indicated by an arrow (A). Filled symbols designate affected individuals and consanguineous loops are indicated by double lines. Microsatellite markers are boxed and the disease-associated haplotype is shaded.

(C) Two-point LOD scores for chromosome 18 markers in the two LAH pedigrees combined. For markers with LOD scores exceeding 3, the Z_{max} is underlined. The position for each marker is indicated in centimorgans (cM), according to the Marshfield genetic map (http://research.marshfieldclinic.org/genetics/).

(D) Multipoint LOD scores in the two LAH pedigrees combined. The relative position of each marker in cM and the LOD score values are indicated on the X and Y axis, respectively.

Comparative Genomics Reveals Synteny with the *lanceolate hair* Phenotype

The *LAH* syntenic region on mouse chromosome 18 contains the locus for an autosomal recessive mutation, *lanceolate hair* (*lah*), and also harbors the desmosomal cadherin cluster (Montagutelli et al., 1996). *lah/lah* pups develop only a few short, fragile hairs on the head and neck which disappear within a few months. The vibrissae are short and abnormal and the pups have thickened skin. Mutant *lah/lah* mice do not exhibit any growth retardation relative to their unaffected littermates (Figures 2E and 2F). A second allele of *lanceolate hair*, named lah^J, later arose as a spontaneous mutation at the Jackson Laboratory (Figures 2G and 2H), and complementation established that the two mutations were allelic (Sundberg et al., 2000). The lah^J/lah^J phenotype is more severe, as the pups fail to grow any normal hairs and completely lack vibrissae. Instead, the pups are covered with abnormally keratinized stubble giving the mouse a "peach fuzz" appearance (Sundberg et al., 2000). Histological analysis of HFs in both *lah/lah* and lah^J/lah^J reveals striking similarities to human LAH (Figures 2I–2L). The main feature is the formation of a swelling above the melanogenic zone. The "bleb" is then pushed up with the progression of the hair growth, leaving the distal end of the hair shaft with a lance-head shape, hence the name *lanceolate hair*. Occasionally, two blebs can be observed within a single anagen follicle (Figure 2M). Degenerative changes in the hair shaft include the loss of the ladder-like pattern of pigment distribution in the medulla, which is replaced by chaotically distributed amorphous pigment granules and air spaces (Figure 2N). In contrast to human LAH patients, the interfollicular epidermis in both mouse *lanceolate* alleles is significantly thickened, exhibiting prominent hyperplasia (Figures 2L and 2M).

Genetic mapping had previously placed the *lah* mutation in the syntenic region of mouse chromosome 18. Mutations in the *Dsg3* gene underlie the *balding* (*bal*) phenotype, and complementation matings indicated

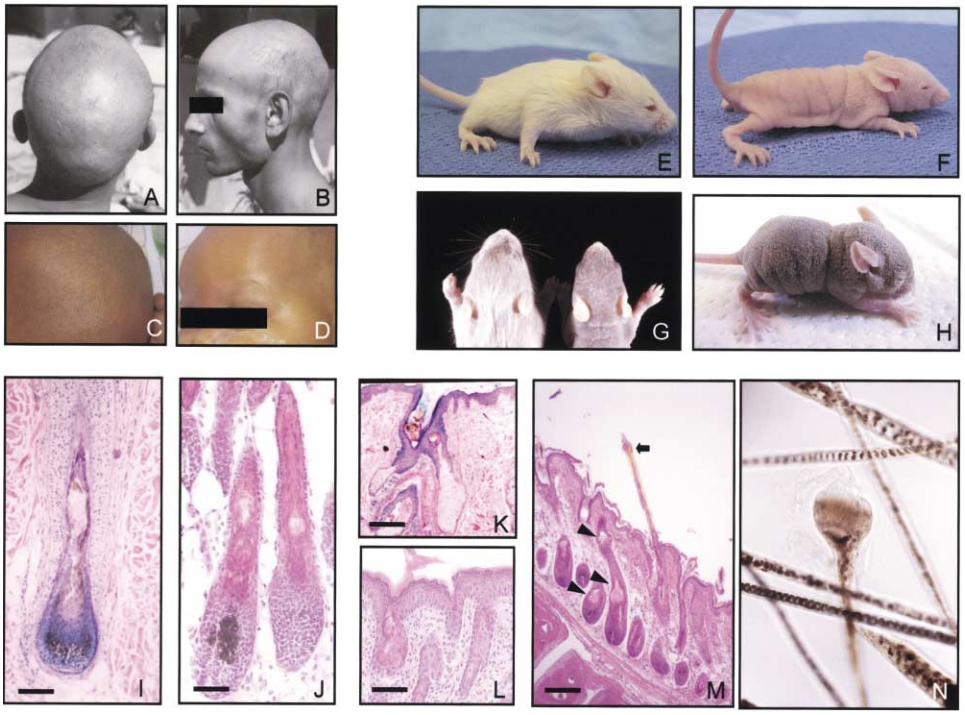

Figure 2. Clinical and Histological Features of the Human LAH Phenotype and the *lanceolate hair* Mouse

(A–D) Clinical presentation of the human LAH phenotype in family LAH-1 (A and B) and LAH-2 (C and D). Note the sparse scalp hair and eyebrows (A and B) and bumpy scalp skin (C and D).

(E–H) Gross abnormalities in the *lanceolate hair* mice. (F) Day 13 *lah/lah* male, with sparse hair on the trunk and abnormal vibrissae. (E) A wild-type day 13 PWK littermate. (G) Day 14 DBA/1lahJ +/+ (left) and lah^J/lah^J (right) male mice. (H) The mutant mouse is bald, runted, and has thickened, folded skin. Vibrissae are completely absent.

(I–L) Skin histology (H&E) from affected patients (I and K) and day 8 lah^J/lah^J (J and L). The formation of a bulbous "bleb" (I and J) and the presence of curled ingrown hair shafts within the hair follicle (K and L) are observed in both human and mouse. Hyperplastic interfollicular epidermis and HF infundibulum are observed in lah^J/lah^J skin (L), but not in human LAH skin (K).

(M) Hair fiber emerging from the skin of a 2-month-old DBA/1lacJ lah^J/lah^J mutant female. Note the bulbous swelling at the tip where the fiber has broken off (arrow). The adjacent anagen hair follicles all have bulbous degenerative changes (arrowheads).

(N) Bright-field illumination of *lah/lah* hairs. Note the bulbous degenerative changes at the breakpoint in the hair. Scale bars: (I) and (M), 75 μm; (J), 40 μm; (K), 100 μm; (L), 60 μm.

that *bal/bal* and *lah/lah* are not allelic (Montagutelli et al., 1996). We screened the remaining desmosomal cadherin genes, and detected no mutations or differences in mRNA levels.

Desmoglein 4, a Member of the Cadherin Superfamily

Unexpectedly, in the process of detailed genomic analysis in the mouse, we identified three previously undescribed cadherin genes within the cluster (Figure 3A). Two of these, *Dsg1*β and *Dsg1*γ, are not found in the human genome, and are reported elsewhere (Kljuic and Christiano, 2003; Pulkkinen et al., 2003). The third cadherin was also present in the human genome, and was designated desmoglein 4 in mouse (*Dsg4*) and human (*DSG4*) (Figures 3A–3D), which share 79% and 86% amino acid identity and homology, respectively. A comparison of the structural organization and homology analysis of DSG4 to the other desmogleins is depicted in Figures 3B–3D. The human and mouse mRNA were highly expressed in skin (Figures 3E and 3F), and together with its colocalization within the *lanceolate* and *LAH* linkage intervals, desmoglein 4 became a candidate gene for both phenotypes.

Dsg4 Is Mutated in Human LAH and *lanceolate hair* Mice

We identified an identical homozygous intragenic 5 kb deletion in affected individuals from both LAH families by direct sequencing (Figures 4A and 4B). The deletion begins 35 nucleotides upstream of exon 5 and ends 289 nucleotides downstream of exon 8. This mutation, designated EX5_8del, generates an in-frame deletion creating a predicted protein missing amino acids 125–335.

Sequence analysis of *Dsg4* in lah^J/lah^J animals revealed a homozygous single base insertion following nucleotide 746 within exon 7, designated 746insT (Figure 4C). The frameshift creates a premature termination codon three codons downstream from the insertion (Figure 4D). RT-PCR data show that the mutant mRNA undergoes nonsense mediated decay, as we were unable to detect any *Dsg4* mRNA (Figure 4F) (Frischmeyer and Dietz, 1999). Sequence analysis of *Dsg4* in *lah/lah* animals identified a homozygous A-to-C transversion at nucleotide 587. This mutation converted a tyrosine residue (TAC) in exon 6 to a serine residue (TCC), designated Y196S (Figure 4E). Y196 is conserved in the majority of desmosomal cadherins, as well as classical cadherins

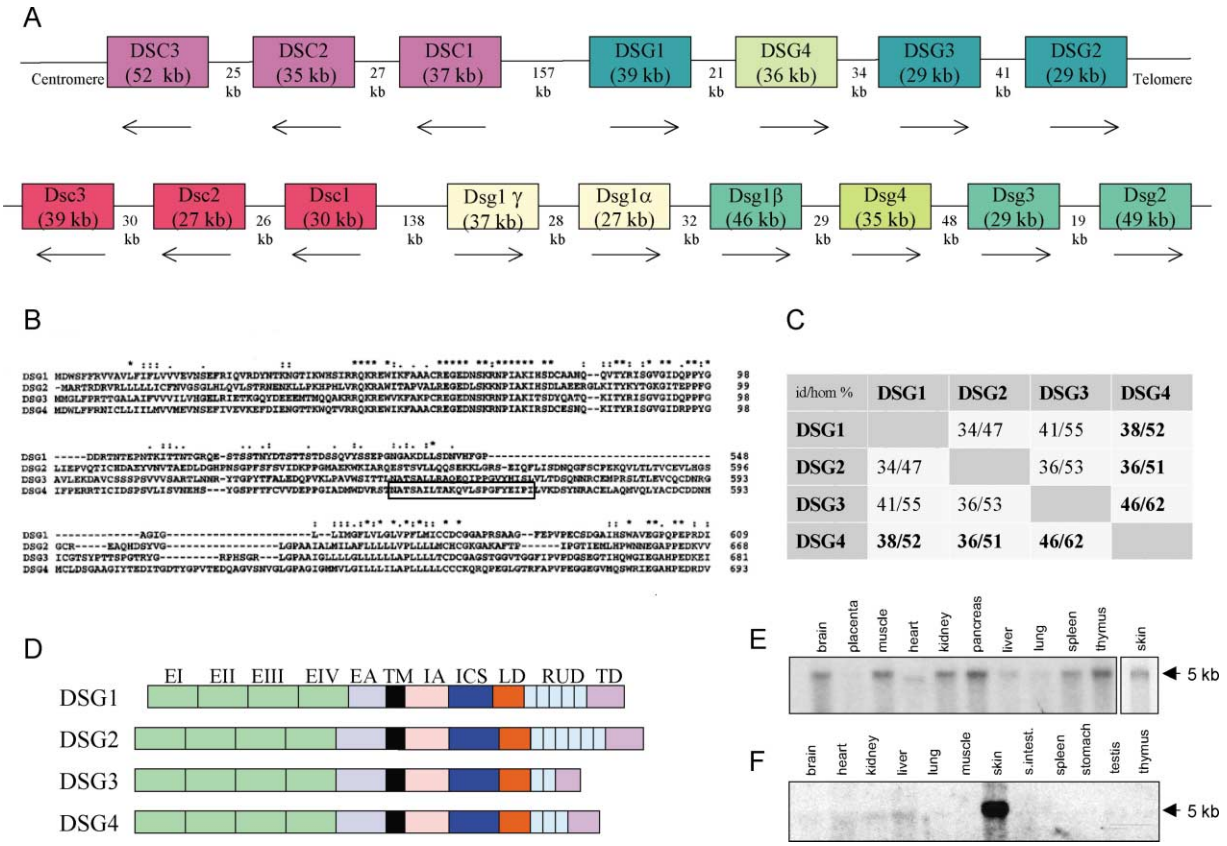

Figure 3. Genomic Organization and Expression Analysis of Desmoglein 4

(A) Genomic structure of the human (top) and mouse (bottom) desmosomal cadherin gene clusters on chromosome 18. The approximate sizes of genes and intragenic regions are indicated in kb, according to the UCSC freezes of December 01 (human) and February 02 (mouse).

(B) Amino acid sequence alignment of representative fragments of human DSG1-4. The peptide sequence against which the antibody was raised is boxed. Asterisks indicate identical residues.

(C) Amino acid identity and homology between DSG1-4. GenBank accession numbers for *DSG4* and *Dsg4* are AY227350 and AY227349.

(D) Comparison of domains among human desmoglein proteins. Note the highly conserved protein structure among all desmogleins, with the exception of the RUD. EI-IV, extracellular cadherin repeats; EA, extracellular anchor domain; TM, transmembrane domain; IA, intracellular anchor; ICS, intracellular cadherin sequence; LD, intracellular linker domain; RUD, repeated unit domain; TD, terminal domain.

(E–F) Northern analysis of human (E) and mouse (F) desmoglein 4.

such as E- and N-cadherin (Figure 4G) and protein prediction software suggested that it represents a potential phosphorylation site. Extensive BLAST searches and sequencing of additional mouse strains indicated that Y196S is not a polymorphism. Thus, the *lah*^{J}/*lah*^{J} mouse serves as a null mutant animal model, whereas the *lah*/*lah* mouse represents a hypomorph. The revised designation of the mouse mutations is *Dsg4*^{lah}/*Dsg4*^{lah} and *Dsg4*^{lahJ}/*Dsg4*^{lahJ}.

Dsg4 Is the Principal Desmosomal Cadherin in the Hair Follicle

In situ hybridization of mouse skin sections and vibrissae follicles revealed that *Dsg4* is expressed in anagen stage HFs. The mRNA was localized to the cells of the matrix, precortex, and IRS of vibrissae HF (Figure 5A). DSG4 was also detected within anagen follicles where its expression commenced in the matrix and extended throughout precortical cells and IRS (Figure 5C). The presence of desmoglein 4 in the inner layer of the HF, where DSG1 (Figure 5D), DSG2, and DSG3 (Kurzen et al., 1998) are absent, suggests a critical role for desmoglein 4 in differentiation of the ascending HF layers.

Desmoglein 4 Is Expressed in Suprabasal Epidermis and Is a Target of PV Autoantibodies

Immunofluorescent labeling of human scalp sections with DSG4 antibody revealed cell border localization of the protein within the suprabasal layers of the epidermis, where it is highly expressed (Figures 5E and 5F). To test the hypothesis that DSG4 could serve as an autoantibody in PV similar to DSG1 and 3, we reacted sera of two PV patients with active skin and oral lesions against a recombinant N-terminal protein of DSG4, demonstrating that DSG4 is also an autoantigen in PV (Figure 5G).

Desmosomes Are Defective in *lah*^{J}/*lah*^{J} Mutants

Transmission electron microscopy of day 14 epidermis and HF from *lah*^{J}/*lah*^{J} mutant pups established the central role of Dsg4 in cell-cell adhesion. At low magnification, acantholysis along cell-cell borders was evident in all layers of mutant epidermis (Figures 5H and 5I). The

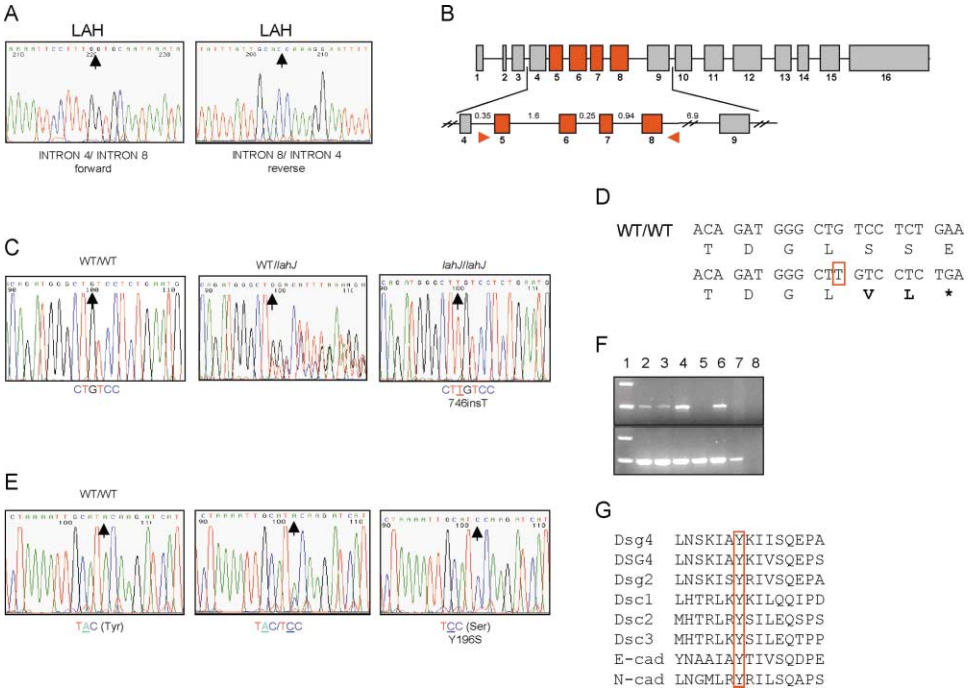

Figure 4. Mutation Analysis in Human and Mouse Desmoglein 4

(A and B) *DSG4* deletion in patients from pedigrees LAH-1 and LAH-2. (A) The deletion breakpoint is between introns 4 and 8 in both LAH pedigrees. (B) Schematic representation of the deletion in LAH patients. The size of the introns is in kb.

(C–G) *Dsg4* mutations in *lah*^{J}/*lah*^{J} (C and D) and *lah*/*lah* (E and G). *lah*^{J}/*lah*^{J} mice were homozygous for a 1 bp insertion in exon 7 (C), which creates a frameshift and premature termination codon three codons downstream (D). (E) Sequence analysis of *Dsg4* in *lah*/*lah* mice revealed a homozygous missense mutation, Y196S, in exon 6. (G) Y196 is conserved among different cadherin proteins.

(F) RT-PCR analysis of skin mRNA from *lah*^{J}/*lah*^{J} and *lah*/*lah* showed presence of the mutant transcript in *lah*/*lah*, but complete lack of *Dsg4* expression in *lah*^{J}/*lah*^{J}. Amplification of *Dsg3* is shown on the lower panel for comparison. Lanes: 1, marker; 2 and 3, PWK +/+; 4 and 6, *lah*/*lah*; 5 and 7, *lah*^{J}/*lah*^{J}; and 8, blank control.

junctions between adjacent keratinocytes in *lah*^{J}/*lah*^{J} revealed complete detachment in some areas, and small, poorly formed desmosomes in others, into which filaments were only scantily inserted (Figures 5J and 5K). Spaces between detached mutant keratinocytes revealed areas in which desmosomes have been torn away from their cells (Figures 5L and 5M). Ultrastructural defects in keratinization of the inner layers of the hair shaft were evident in mutant HFs, consisting of a disorganized array of air spaces and pigment granules in the medulla (Figure 5N), and the complete detachment of keratinocytes in Henle's and Huxley's layers and the cortex. The cells are severed from their neighbors, leaving behind a row of detached desmosomes (Figure 5O).

lah^{J}/*lah*^{J} Epidermal Keratinocytes Exhibit a Hyperproliferative Phenotype

In order to further characterize the hyperplastic changes within the skin of mutant animals, we first assayed the expression of several epidermal markers. K5 was ubiquitously and evenly expressed in the basal layer of WT skin, compared to a patchy pattern of expression with fewer strongly positive basal cells in *lah*^{J}/*lah*^{J} mutants (Figures 6A and 6B). The hyperproliferation marker K6 was significantly overexpressed in the spinous layer of the epidermis and HF infundibulum of mutant animals (Figures 6C and 6D). The expression of α6 integrin, a hemidesmosomal marker, was markedly reduced in the basal layer of the interfollicular epidermis of the mutants (Figures 6E and 6F). Expression of involucrin, loricrin, K1, Dsc1,2,3; Dsg1,3; β catenin; E-cad; P-cad; Pkp1; Dsp; and Pg were unchanged between WT and mutant animals (not shown).

In mutant epidermis, the finding of patchy K5 staining, the presence of K6 and the reduced expression of α6 integrin were all consistent with premature or accelerated exit of keratinocytes from the basal compartment. Consistent with the hypothesis that the proliferative compartment might therefore be expanded, we detected a higher number of PCNA expressing keratinocytes in the basal epidermis of *lah*^{J}/*lah*^{J} animals, as well as the existence of ectopically proliferating cells in the suprabasal layers (Figures 6G and 6H). To further investigate the nature of the hyperproliferative phenotype, we assayed the expression of β1 integrin and EGFR and found that both were ectopically expressed in the suprabasal layers of mutant epidermis (Figures 6I–6L), while we found no difference in the expression pattern of total or activated MAP kinase (not shown). TUNEL staining was performed to assess the extent of apoptosis in mutant epidermis and HF, and no differences were detected compared to control animals (not shown).

Cell attachment kinetics of primary epidermal keratinocytes were performed to further characterize the skin of *lah*/*lah* mice. Attachment assays showed greater than 2-fold enhanced attachment of *lah*/*lah* keratino-

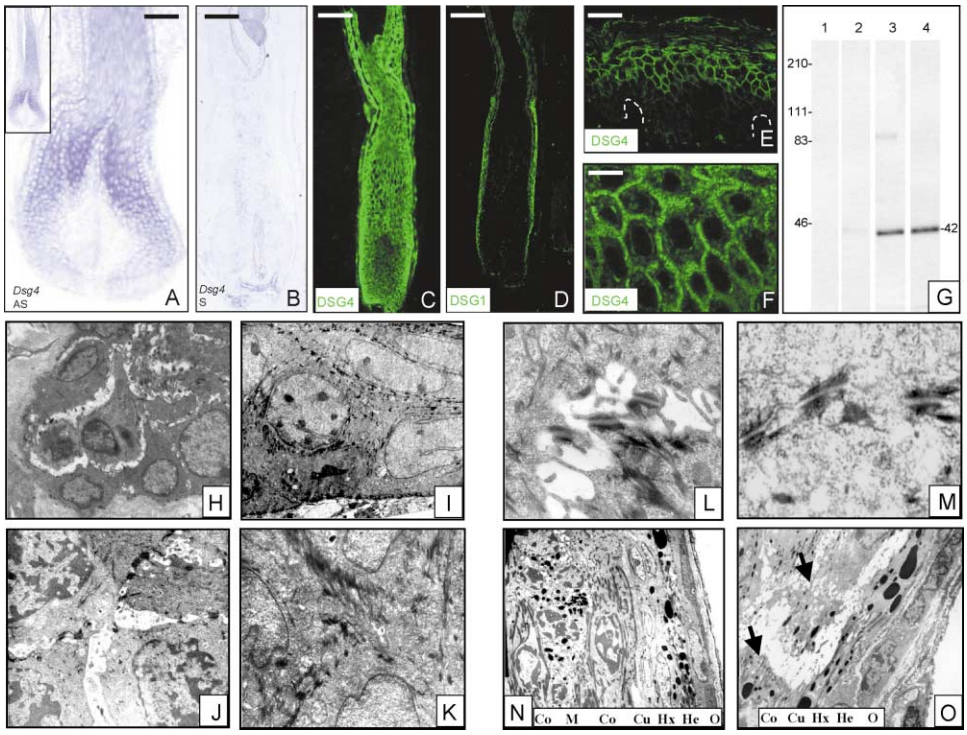

Figure 5. Desmoglein 4 Expression and Ultrastructural Defects in *lah^{J}/lah^{J}* Skin

(A) In situ hybridization of mouse *Dsg4* in vibrissa shows a strong signal in the upper matrix. (B) Control sense probe. (C) Immunofluorescence staining of human DSG4 in dissected human scalp follicle shows intense staining in the IRS and all layers of the matrix and precortex. (D) In contrast, DSG1 expression is localized only to the IRS. (E and F) DSG4 immunostaining in interfollicular epidermis reveals a strong positive signal in the suprabasal layers. (G) PV autoantibodies recognize DSG4. Lanes 1 and 2 were stained with sera from a healthy male and female subjects with no history of skin disease. Lanes 3 and 4 were stained with sera from two different PV patients with active lesions at the time serum was obtained. Sera recognize a recombinant protein of N-terminal region of DSG4 (42 kDa). (H–O) Dysadhesion between all keratinocyte layers in day 14 mutant epidermis (H) compared to WT epidermis (I) with tight adhesion between cells (4000×). (J) Loss of connection between four adjoining suprabasal keratinocytes reveals sparse poorly formed desmosomes between cells, with scant insertion of filaments as compared to WT cells (K) (7500×). (L) High magnification of desmosomes that have been torn away from adjacent keratinocytes compared to intact desmosomes (M) in WT skin (15,000×). (N) Disorganization of the medulla in the area just above the dermal papilla in a day 14 *lah^{J}/lah^{J}* mutant animal, while the concentric layers of the hair shaft and IRS still appear largely normal (2500×). (O) Higher up the HF, adjoining keratinocytes within the IRS layers are now torn apart, leaving behind rows of desmosomes along previously adherent cell borders (arrows) (4000×). O, outer root sheath; M, medulla; Co, cortex; Cu, Cuticle of cortex; Hx, Huxley's layer; and He, Henle's layer. White dashed lines demarcate the dermal-epidermal junction. Scale bars: (A), 50 μm; (B), (C), and (D), 100 μm; (E), 60 μm; and (F), 10 μm.

cytes (21.7 ± 1.8% of total seeded cells), compared to WT (9.0 ± 2.1%) after 24 hr in culture on vitrogen-fibronectin-coated dishes (Figures 6M–6O). In this respect, it is noteworthy that *lah/lah* keratinocytes were also able to attach to uncoated plastic dishes, while the WT keratinocytes failed to do so. *lah/lah* keratinocytes formed fully confluent monolayers by day 4 of culture in low Ca^{2+}, whereas the WT keratinocytes reached only 60%–70% confluency during the same period, suggesting an enhanced ability of *lah/lah* cells to spread, explaining why they precociously form monolayers in culture. Since epithelial sheets do not form in low Ca^{2+} conditions, we compared the response of *lah/lah* and WT keratinocytes when both are induced to differentiate in high Ca^{2+} medium. Upon switching to high Ca^{2+} conditions, the mutant keratinocytes behaved similar to WT cells and no morphological differences were seen for up to 3 weeks. We assayed the expression levels and assembly status of intermediate filament and adhesion components in primary cultured keratinocytes, and found no differences in K5, Dsg1, Pg, Pkp1, or actin (not shown).

lah^{J}/lah^{J} Hair Matrix Keratinocytes Exhibit Disrupted Differentiation

The transition from proliferation to differentiation in the lower HF occurs along a gradient as cells pass through the line of Auber. In WT matrix keratinocytes, we observed the expected graduation from the base of the follicles, where all cells are proliferating, to the precortex, where essentially all cells are differentiating (Figures 7A and 7B). Strikingly, in mutant HF, we instead observed a dramatic cessation of proliferation and an abrupt transition to differentiation between adjacent cells (Figures 7A and 7B). The premature loss of the proliferative signal and sudden switch to differentiation occurs precisely in the region of cell-cell separation (Figures 7C and 7D) and the onset of the formation of the lance head.

We then assessed the expression of hoxC13 and the hair keratins hHb2 and hHa4, which are specific for hair shaft cuticle and cortex differentiation, respectively. While both proteins are expressed in mutant follicles, their expression is spatially restricted compared to WT follicles. In WT follicles, both proteins are expressed in

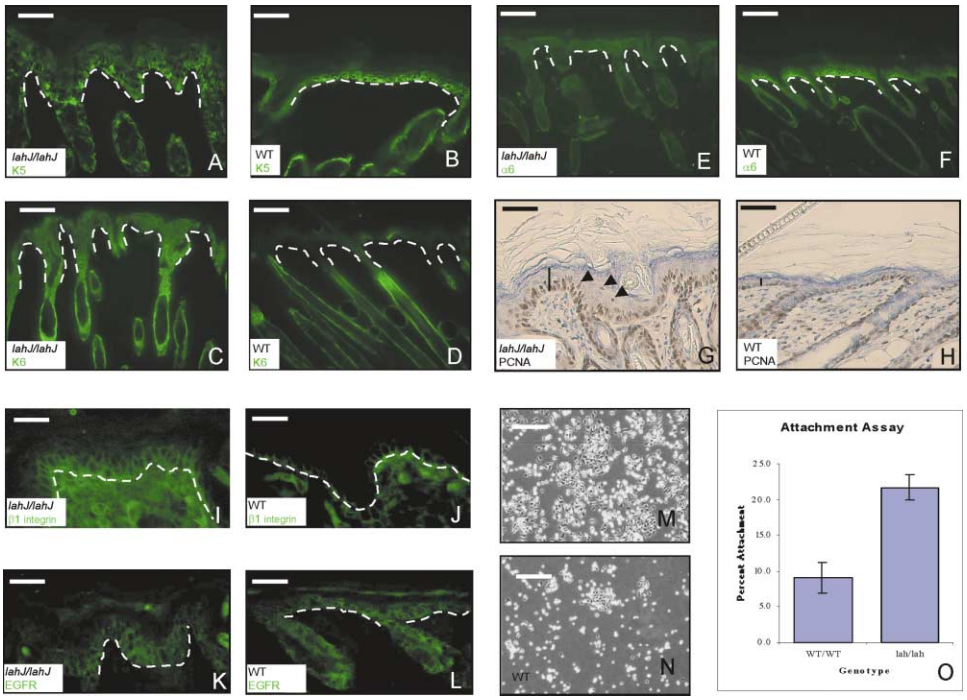

Figure 6. Activation of Epidermal Keratinocytes in *lah*/*lah* and *lah*^{J}/*lah*^{J} Mutant Skin

(A–H) Comparison of different proliferation and differentiation markers between day 8 *lah*^{J}/*lah*^{J} and WT epidermis. (A and B) K5 immunofluorescence shows patchy expression in basal cells of *lah*^{J}/*lah*^{J} epidermis. K6 is ubiquitously expressed in *lah*^{J}/*lah*^{J} epidermis and infundibulum of HF (C), while WT epidermis is negative (D). (E and F) α6 integrin, a hemidesmosomal component, is markedly reduced in *lah*^{J}/*lah*^{J} basal epidermis. (G and H) PCNA immunohistochemistry shows a higher number of positive staining cells in the thickened (brackets) *lah*^{J}/*lah*^{J} epidermis (G) compared to WT (H). Suprabasal β1integrin (I and J) and EGFR (K and L) in mutant versus WT epidermis. *lah*/*lah* epidermal keratinocytes exhibit enhanced attachment and spreading after 24 hr in culture (M) relative to WT keratinocytes (N). (O) Quantitative measurement of the fraction of attached cells in (M) and (N). Error bar: standard error of the mean (SEM). White dashed lines demarcate the dermal-epidermal junction. Scale bars: (A), (B), (G), and (H), 32 μm; (C), (D), (E), and (F), (M), and (N) 40 μm; (I), (J), (K), and (L), 25 μm.

the upper bulb and in the middle portion of the HF, whereas in mutant HF they are restricted to a much smaller zone at the bulb narrowing (Figures 7F–7I). HoxC13 regulates the expression of early hair keratins and is normally expressed in upper matrix/lower precortex, above the zone of hHa4 expression, as well as in the hair cuticle (Figure 7G). In mutant skin, hoxC13 is significantly reduced in the lower hair follicle and is nearly undetectable in the cuticle (Figure 7K).

Discussion

While many examples of correlations of human disorders with mouse models exist in the literature, there are very few which represent pure forms of alopecia without ectodermal dysplasia. We established the close correlation of the *hairless* mouse phenotype with atrichia with papular lesions (Ahmad et al., 1998) and the *nude* mouse phenotype with congenital alopecia and T cell immunodeficiency (Frank et al., 1999), both of which result from defects in transcription factors. To our knowledge, there have been no reports to date of defects in structural proteins in mice that closely mimic a human hair disorder (Tong and Coulombe, 2003). LAH and *lanceolate hair,* therefore, represent corresponding human and mouse phenotypes resulting from defects in a structural component of the epidermis and HF, desmoglein 4. The biological relevance of these findings extends into the area of skin autoimmunity, since we show that DSG4 also serves as an autoantigen in patients with PV (Nguyen et al., 2000). We have used both a naturally occurring null mutant (*lah*^{J}/*lah*^{J}) and hypomorphic (*lah*/*lah*) mouse model to begin dissecting the role of Dsg4 in epidermal and HF homeostasis and disease. Our findings demonstrate a central role of desmoglein 4 in keratinocyte cell adhesion, and furthermore, in coordinating cellular dynamics in the lower HF during the switch from proliferation to differentiation.

Dsg4 Is Critical for Intercellular Adhesion and Keratinocyte Differentiation

Our ultrastructural results suggest that desmoglein 4 participates in a desmosomal junction with a highly specialized function during hair shaft differentiation. The three-dimensional architecture of the HF itself imparts critical positional information to the cellular dynamics of hair growth, and as such, the maintenance of cell attachment is particularly critical during differentiation (Bullough and Laurence, 1958; Van Scott et al., 1963). The HF layers (Figure 7E) are morphologically distinct, desmosome-rich, cylindrical epithelial sheets that keratinize in a temporally autonomous pattern during anagen, and are each characterized by a distinct signature of hair keratins. The rate of mitosis below the line of Auber must be precisely synchronized with the switch to differentiation, so that specific programs are executed at

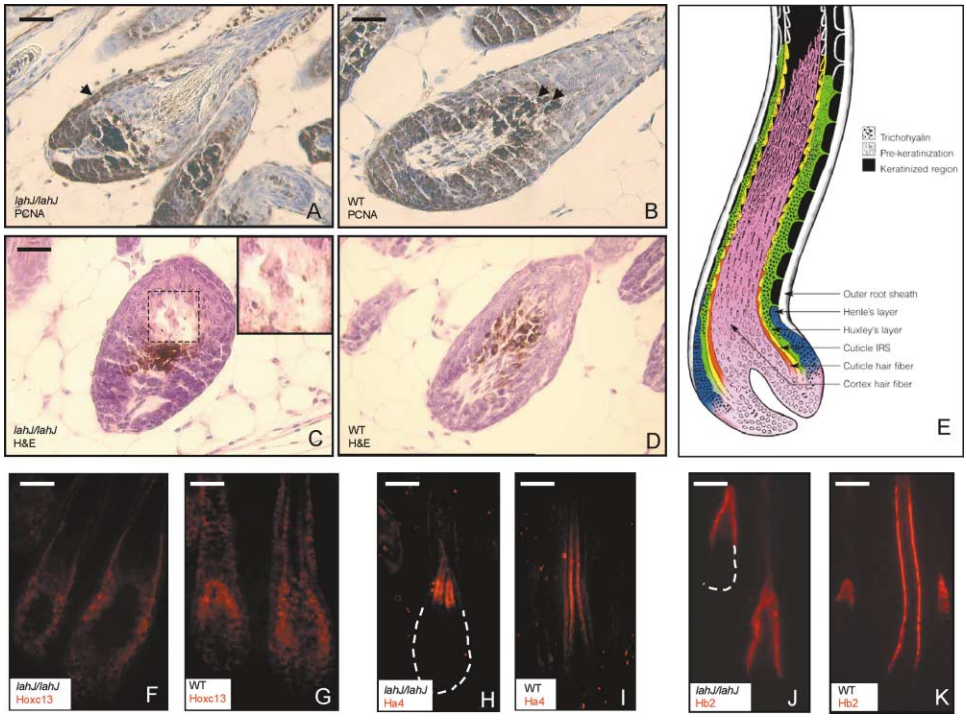

Figure 7. *lah^{J}/lah^{J}* Hair Matrix Keratinocytes Display Perturbations in the Switch from Proliferation to Differentiation

(A and B) PCNA immunohistochemistry reveals an abrupt transition from proliferation (brown) to differentiation (blue) as compared to the gradual transition in a WT follicle. This occurs in a region of cell-cell separation (C) compared to the tight adhesion between cells of a WT follicle (D). (E) Schematic of HF showing the concentric layers and keratinization patterns (modified from Auber, 1952). (F–K) Downregulation and misexpression of hair keratins and hoxC13. HoxC13 expression is reduced in *lah^{J}/lah^{J}* matrix/precortex cells (F) compared to WT skin (G). hHa4 (H and I) and hHb2 (J and K) hair keratins specific for hair shaft cortex and cuticle, respectively, show spatially reduced expression in *lah^{J}/lah^{J}* follicles. White dashed lines demarcate the borders of the HF. Scale bars: (A), (B), (C), and (D), 20μm; (F–K), 45 μm.

the correct time within a given layer (Auber, 1952). Further, as the differentiating cells of the precortex are forced upward through the narrow neck of the "funnel" created by the external HF membranes, they are under considerable mechanical pressure (Bullough and Laurence, 1958; Van Scott et al., 1963). We provide evidence that the requirement of HF keratinocytes to smoothly transition from proliferation to differentiation (Figures 7A and 7B), to resist shear forces as they ascend (Figures 2, 5, and 7), and to differentiate along a different pathway than their neighbor (Figures 7F–7K) is critically dependent on cell-cell attachment mediated in part by desmoglein 4.

Absence of Dsg4 Leads to Epidermal Hyperproliferation

Our initial histological observations of mutant epidermis revealed marked thickening and hyperplasia, which prompted us to more closely examine the mechanism by which this occurred. Mutant epidermis revealed a profile of alterations consistent with an activated keratinocyte phenotype, specifically, downregulation of α6 integrin and K5 in the basal layer, suggesting a premature exit from the basal compartment. We detected marked upregulation of K6 throughout mutant epidermis (Figure 6C), as well as a prominent increase in the number of PCNA-positive proliferating cells in the basal and suprabasal layers. We next asked whether this phenotype might be accompanied by the classical mediators of this phenomenon (Rikimaru et al., 1997), and found that both β1 integrin and EGFR were ectopically expressed in the suprabasal layers in mutant epidermis (Figures 6H–6K). In the context of *lanceolate hair* mutant animals, the triad of PCNA, β1 integrin, and EGFR in the suprabasal cells correlates with defective cell adhesion in the epidermis. Additionally, the absence of nuclear MAPK in hyperproliferative epidermis suggests that in *lah/lah* mutants, EGFR may be signaling via an alternate pathway. Although the causes versus effects of suprabasal integrin expression are incompletely understood at present, the examples reported to date have been associated with an inflammatory response (Carroll et al., 1995). *lah/lah* mutant animals exhibit all the hallmarks of this response in the absence of inflammation, suggesting that the two events may be separable. Since K6 represents a transcriptional target of EGFR signaling (Jiang et al., 1993) and is strongly upregulated in mutant epidermis, it is likely that the hyperproliferative phenotype in *lah^{J}/lah^{J}* mutants is mediated by activation of additional EGF target genes.

The unexpected finding of several key hyperproliferative markers in the epidermis led us to more closely investigate the proliferative properties of both epidermal and HF cells in *lanceolate hair* mutant animals. Quantitation of cellular kinetics revealed that *lah/lah* primary mouse keratinocytes exhibited enhanced cell spreading

in addition to attachment, typical of activated or wound healing keratinocytes (Freedberg et al., 2001; Grinnell, 1990). One explanation for these findings is simply that in the absence of correct cell-attachment, the cells exhibit characteristics of activated keratinocytes. A similar mechanism was recently proposed for the enhanced attachment phenotype of keratinocytes from a patient with mutations in plectin, a hemidesmosomal component (Kurose et al., 2000). It is well established that transient alterations of EGFR expression and activation are known to have profound effects on keratinocyte attachment, spreading and migration particularly during wound healing (Hudson and McCawley, 1998). Consistent with its overexpression in the epidermis, we hypothesize that the cell kinetic behavior of *lah/lah* mutant keratinocytes is also mediated by the activation of genes downstream of EGFR.

What Makes a *lanceolate* Hair?

The most striking aspect of the *lanceolate hair* phenotype is a transient, intermittent defect in differentiation of the HF precortical cells. Early in anagen, the growing follicles at first appear essentially normal, until some cells undergo a marked engorgement in the precortex region, resulting in a bleb within the hair shaft. In the center of the bleb, cells are torn away from their neighbors (Figures 7C and 7D), and subsequently undergo premature, abnormal, and rapid keratinization.

What is the mechanism by which absence of desmoglein 4 results in perturbed differentiation of HF keratinocytes? Emerging evidence suggests that the adhesive role of intercellular junctions, such as desmosomes, may in and of itself confer enhanced signaling by bringing apposing cell membranes into closer proximity, thereby facilitating other types of connections such as communicating junctions and ligand/receptor interactions (Jamora and Fuchs, 2002). Such interactions impact upon the diffusion of secreted factors across cell membranes and facilitate the establishment of morphogen gradients by positioning of their cognate transmembrane receptors. Importantly, cell adhesion molecules provide support for the extracellular matrix proteoglycans between cells that are required for transmission of signals such as Wnts and BMPs (Paine-Saunders et al., 2002).

One explanation for the origin of the *lanceolate* hair is that the abnormal precortical cells in *lanceolate* HF represent a population of naïve keratinocytes that have been incompletely programmed upon their exit from the proliferation zone. We have shown by PCNA expression in mutant HF that the transition from proliferation to differentiation is dramatically disturbed, and that rather than proceeding along a gradient, instead it occurs abruptly (Figures 7A and 7B). Given the complexity of signaling programs that are active in this region, including BMPs, Wnts, and Notch/Delta, it is likely that the primary defect in cell adhesion also precipitates the inability of these signaling molecules to fully execute cell fate determination in this region. Evidence in support of this hypothesis includes perturbed expression of hoxC13 and the cuticle and cortex hair keratins in mutant animals (Figure 7), all three of which are downstream markers of both BMP and Wnt signaling in the HF precortex (Kulessa et al., 2000). The uncoupling of the transition from proliferation to differentiation further demonstrates that the transmission of survival signals is disrupted in the absence of intact cell-cell adhesion. What results then is a total communication breakdown in the lower HF, resulting in failed execution of differentiation programs as a result of defective desmosomal adhesion.

Jamora and Fuchs recently put forth the notion that the differential expression of desmosomal cadherins in the epidermis and HF imply a broader function for these proteins than simply as a "clamp between two cells" (Jamora and Fuchs, 2002). Likewise, the authors of the original description of the *lanceolate hair* mouse had postulated that *"…a defective interaction between hair follicle adhesion molecules and keratins,"* and moreover that *"…a normal signaling molecule is missing or abnormal that periodically stimulates the follicle to continue in anagen"* (Sundberg et al., 2000), thus predicting both a structural and a communication defect in the *lanceolate* HF.

We have uncovered a pivotal role for desmoglein 4 in keratinocyte cell adhesion, and moreover, in the execution of differentiation programs within the innermost keratinocyte populations of the HF, where the processes of mitosis, cell fate determination, and intercellular adhesion must be seamlessly coordinated.

Experimental Procedures

Linkage Analysis

Blood samples from family members were collected following informed consent, and genomic DNA was extracted using the PureGene DNA Isolation Kit (Gentra Systems). Microsatellite markers were chosen from the Marshfield genetic map (http://research.marshfieldclinic.org/genetics/). A fully penetrant recessive model with no phenocopies and disease allele frequency of 0.001 was assumed. Marker alleles were recoded using the RECODE program (ftp://watson.hgen.edu/pub/recode.tar.Z). Two-point analyses were carried out using the MLINK program of the FASTLINK suite of programs (Lathrop et al., 1984) and multipoint and haplotype analyses using the SIMWALK program version 2.82 (Sobel and Lange, 1996). Recombination distances between markers were obtained from the sex-averaged Marshfield genetic map.

Genomic Structure of Desmoglein 4

We analyzed the region on mouse chromosome 18 containing the desmosomal cadherin cluster (http://genome.ucsc.edu/; February 2002 Freeze). Analysis of three open reading frames, Ensembl 00000037563, Geneid CHR18_197, and Genscan CHR18_2.430, was used to predict the genomic structure of *Dsg4*. Sequencing of cDNA from mouse skin RNA and genomic DNA of PWK strain confirmed the sequence and identified an additional exon. The final cDNA sequence of *Dsg4* was deposited under GenBank accession number AY227349.

Using the BLAT sequence analysis tool at http://genome.ucsc.edu/ (December 2001 Freeze), we identified four human gene predictions homologous to the mouse *Dsg4* cDNA within the human desmosomal gene cluster. Two of them, Ensembl ENST00000280910 and Fgenesh^{2+} C18000296, were used to assemble a human *DSG4* gene prediction. The final sequence was confirmed by sequencing of cDNA from human epithelial RNA and from genomic DNA, and is deposited under GenBank accession number AY227350. Amino acid identity and homology values were calculated using the NCBI blastp software (http://www.ncbi.nlm.nih.gov/BLAST/). For alignment of the four human desmoglein amino acid sequences, we used the Clustal X software (Thompson et al., 1999).

Mutation Screening and RT-PCR

All exons and splice sites were PCR amplified from genomic DNA from human LAH patients and controls, as well as *lah/lah*, *lah^J/lah^J*,

and control animals. PCR products were directly sequenced in an ABI Prism 310 sequencer. *Dsg4* cDNA was RT-PCR amplified from control and mutant whole skin RNA using the following primers: Dsg4 cDNA1F (5′-TCTCCTAGTACAGCCTGCTT-3′) and Dsg4 cDNA5R (5′-AGTGGTCTCTCCAAGTCTTC-3′), corresponding to the first five exons of *Dsg4*. The potential phosphorylation of Y196 was predicted using software available at www.cbs.dtu.dk/services/NetPhos/.

Northern Analysis and In Situ Hybridization

Two μg normal human skin poly(A) RNA (Stratagene) was transferred to Nylon membranes (Amersham) (Sambrook et al., 1989). Human and mouse multiple tissue blots containing 2 μg poly(A) RNA per lane were purchased from Ambion and OriGene Technologies INC, respectively. The human blots were hybridized with ^{32}P-labeled cDNA probe corresponding to human *DSG4* exons 3–8 amplified using primers DSG4 cDNA3F (5′-AGTTTGCCGCAGCCTGTCGA-3′) and DSG4 cDNA8R (5′-CCAGTTATCAGTGCCTTCTTC-3′). The mouse blots were hybridized with a ^{32}P-labeled cDNA probe corresponding to *Dsg4* exons 4–8 amplified using primers Dsg4 cDNA 4F (5′-TTGATCGGCCACCTTACGG-3′) and Dsg4 cDNA 8R (5′-CCAACCAGTTATCAGTGCCT-3′). The hybridizations were carried out using Rapid Hyb buffer (Amersham).

In situ hybridization was performed on 4% PFA fixed 4 μm frozen sections from Balb/c adult mice with DIG labeled *Dsg4* riboprobes (Roche Molecular Biochemicals), as described elsewhere (Mendelsohn et al., 1999). After developing the signal with NBT/BCIP substrate, slides were dehydrated and mounted in Shandon mounting medium (Thermoshandon).

DSG4 Antibody Synthesis, Immunofluorescence Microscopy, Western Blot

Polyclonal antibodies for human DSG4 were raised in chicken against the following peptide: 'N'-NATSAILTALQVLSPGFYEIPI-'C' (Washington Biotechnology). Other antibodies were as follows: β-catenin (1:100) (Sigma); K1 (1:500), K5 (1:1000), K6 (1:500), loricrin (1:500) involucrin (1:1000) diphosphorylated Erk1/2 (1:50) (Babco); hoxC13 (1:800), Ha4 (1:200) and Hb2 (1:2000) (generous gift from Dr. Jurgen Schweitzer); α6 integrin (1:50), β1 integrin (1:50) (Chemicon), Dsg1 (1:100), Dsg3 (1:30), P-cadherin (1:50), and EGFR (1:50), Erk1/2 (1:100) (Santa Cruz); E-cad (1:50) (BD Transduction laboratories); Pg (1:50) and Pkp1 (1:100) (Zymed); PCNA (1:50) (Oncogene Research Products); Dsp (1:20) and pan-desmocollin (1:50) (generous gift from Dr. My Mahoney); nude (Foxn1) (1:30) (generous gift from Dr. Janice Brissette).

Human scalp and mouse dorsal skin sections of day 8 *lah^J/lah^J* or WT littermates were fixed in either acetone at −20°C for 10 min or 4% PFA in PBS at room temperature for 10 min. Immunofluorescent staining was performed as described previously for both cells and frozen sections (Harlow and Lane, 1998). For mouse monoclonal antibodies, the M.O.M. kit was used for immunofluorescence and Mouse Elite Kit was used for immunihistochemistry (Vector Laboratories).

Recombinant protein of an N-terminal region of DSG4 was expressed in SG13009 bacteria using pQE30 expression vector (Nguyen et al., 2000). Recombinant protein was affinity purified with Qiagen Ni-NTA Spin column and used for Western blot analysis of sera from PV patients or healthy individuals. Binding of primary antibodies was recognized by HRP-conjugated goat anti-human IgG secondary antibody.

Transmission Electron Microscopy

Skin from dorsal back of day 14 *lah^J/lah^J* and WT littermates was fixed in half-strength Karnovsky's fixative (2% PFA/2.5% glutaraldehyde phosphate buffer) followed by fixation in 1.3% osmium tetroxide. Samples were processed using standard TEM techniques and mounted in Epon resin. Ultrathin sections were collected on grids and stained with uranyl acetate and lead citrate. Sections were visualized using a Jeol 100CX transmission electron microscope.

Primary Mouse Keratinocyte Culture

Mouse keratinocytes were isolated and cultured as described (Morris et al., 1994), with minor modifications. 2×10^6 cells per dish were plated onto 35 mm dishes (Becton Dickinson) with vitrogen-fibronectin coating and cultures were kept in a 32°C humidified incubator. For high Ca^{2+} conditions, a final concentration of 1.2 mM was used on day 4–5 cultures. For immunostains, the cells were fixed in ice-cold methanol at −20°C for 10 min. The attachment assay was performed 24 hr after seeding in low Ca^{2+} medium (Freshney, 1987) on triplicate plates. Cells were trypsinized with 0.25% trypsin for 4 min at 32°C, collected by centrifugation, and counted using a hemocytometer.

Acknowledgments

We thank the family members for their interest and participation in this work. We appreciate discussions with Drs. David Owens, Ronald Liem, Akemi Ishida-Yamamoto, John Mc Grath, Abraham Zlotogorski, Howard Baden, Lloyd King, Elise Olsen, Lowell Goldsmith, and Cathy Mendelsohn. We thank Drs. Gary Struhl and Andreu Casali-Taberner for their generous help with confocal microscopy. We thank Andrew Engelhard, Karima Djabali, Marija Tadin, Hyunmi Kim, Kai Sun, Ming Zhang, Nancy Zhou, and HaMut Lam. This work was supported in part by USPHS NIH R01-44924 (AMC), K26-RR173 (JPS), P01 AR38923 (JU), R03 AR47938 (MGM), and the March of Dimes Birth Defects Foundation (AMC).

Received: February 10, 2003
Revised: March 25, 2003
Accepted: April 1, 2003
Published: April 17, 2003

References

Ahmad, W., ul Haque, M.F., Brancolini, V., Tsou, H.C., ul Haque, S., Lam, H., Aita, V.M., Owen, J., deBlaquiere, M., Frank, J., et al. (1998). Alopecia universalis associated with a mutation in the human hairless gene. Science *279*, 720–724.

Armstrong, D.K., McKenna, K.E., Purkis, P.E., Green, K.J., Eady, R.A., Leigh, I.M., and Hughes, A.E. (1999). Haploinsufficiency of desmoplakin causes a striate subtype of palmoplantar keratoderma. Hum. Mol. Genet. *8*, 143–148.

Auber, L. (1952). The anatomy of follicles producing wool-fibers, with special reference to keratinization. Trans. Roy. Soc. Edinburgh *62*, 191–254.

Bullough, W.S., and Laurence, E.B. (1958). The mitotic activity of the follicle. In The Biology of Hair Growth, W. E. Montagna, ed. (New York: Academic Press), pp. 171–187.

Buxton, R.S., Cowin, P., Franke, W.W., Garrod, D.R., Green, K.J., King, I.A., Koch, P.J., Magee, A.I., Rees, D.A., Stanley, J.R., et al. (1993). Nomenclature of the desmosomal cadherins. J. Cell Biol. *121*, 481–483.

Carroll, J.M., Romero, M.R., and Watt, F.M. (1995). Suprabasal integrin expression in the epidermis of transgenic mice results in developmental defects and a phenotype resembling psoriasis. Cell *83*, 957–968.

Chidgey, M., Brakebusch, C., Gustafsson, E., Cruchley, A., Hail, C., Kirk, S., Merritt, A., North, A., Tselepis, C., Hewitt, J., et al. (2001). Mice lacking desmocollin 1 show epidermal fragility accompanied by barrier defects and abnormal differentiation. J. Cell Biol. *155*, 821–832.

Eshkind, L., Tian, Q., Schmidt, A., Franke, W.W., Windoffer, R., and Leube, R.E. (2002). Loss of desmoglein 2 suggests essential functions for early embryonic development and proliferation of embryonal stem cells. Eur. J. Cell Biol. *81*, 592–598.

Frank, J., Pignata, C., Panteleyev, A.A., Prowse, D.M., Baden, H., Weiner, L., Gaetaniello, L., Ahmad, W., Pozzi, N., Cserhalmi-Friedman, P.B., et al. (1999). Exposing the human nude phenotype. Nature *398*, 473–474.

Freedberg, I.M., Tomic-Canic, M., Komine, M., and Blumenberg, M. (2001). Keratins and the keratinocyte activation cycle. J. Invest. Dermatol. *116*, 633–640.

Freshney, R.I. (1987). Animal Cells: A Manual of Basic Technique. (New York, Wiley-Liss, Inc.).

Frischmeyer, P.A., and Dietz, H.C. (1999). Nonsense-mediated mRNA decay in health and disease. Hum. Mol. Genet. *8*, 1893–1900.

Fuchs, E., Merrill, B.J., Jamora, C., and DasGupta, R. (2001). At the roots of a never-ending cycle. Dev Cell *1*, 13–25.

Garrod, D.R., Merritt, A.J., and Nie, Z. (2002). Desmosomal cadherins. Curr. Opin. Cell Biol. *14*, 537–545.

Green, K.J., and Gaudry, C.A. (2000). Are desmosomes more than tethers for intermediate filaments? Nat. Rev. Mol. Cell Biol. *1*, 208–216.

Grinnell, F. (1990). The activated keratinocyte: up regulation of cell adhesion and migration during wound healing. J. Trauma *30*, S144–149.

Hardy, M.H. (1992). The secret life of the hair follicle. Trends Genet. *8*, 55–61.

Harlow, E., and Lane, D. (1998). Using Antibodies: A Laboratory Manual (Cold Spring Harbor, New York: Cold Spring Harbor Laboratory Press).

Hudson, L.G., and McCawley, L.J. (1998). Contributions of the epidermal growth factor receptor to keratinocyte motility. Microsc. Res. Tech. *43*, 444–455.

Hunt, D.M., Rickman, L., Whittock, N.V., Eady, R.A., Simrak, D., Dopping-Hepenstal, P.J., Stevens, H.P., Armstrong, D.K., Hennies, H.C., Kuster, W., et al. (2001). Spectrum of dominant mutations in the desmosomal cadherin desmoglein *1*, causing the skin disease striate palmoplantar keratoderma. Eur. J. Hum. Genet. *9*, 197–203.

Jamora, C., and Fuchs, E. (2002). Intercellular adhesion, signalling and the cytoskeleton. Nat. Cell Biol. *4*, E101–108.

Jiang, C.K., Magnaldo, T., Ohtsuki, M., Freedberg, I.M., Bernerd, F., and Blumenberg, M. (1993). Epidermal growth factor and transforming growth factor alpha specifically induce the activation- and hyperproliferation-associated keratins 6 and 16. Proc. Natl. Acad. Sci. USA *90*, 6786–6790.

Kljuic, A., and Christiano, A.M. (2003). A novel mouse desmosomal cadherin family member, desmoglein 1γ. Exp. Dermatol. *12*, 20–29.

Kljuic, A., Gilead, L., Martinez-Mir, A., Frank, J., Christiano, A.M., and Zlotogorski, A. A nonsense mutation in the desmoglein 1 gene underlies striate keratoderma. Exp. Dermatol., in press.

Koch, P.J., Mahoney, M.G., Ishikawa, H., Pulkkinen, L., Uitto, J., Shultz, L., Murphy, G.F., Whitaker-Menezes, D., and Stanley, J.R. (1997). Targeted disruption of the pemphigus vulgaris antigen (desmoglein 3) gene in mice causes loss of keratinocyte cell adhesion with a phenotype similar to pemphigus vulgaris. J. Cell Biol. *137*, 1091–1102.

Kulessa, H., Turk, G., and Hogan, B.L. (2000). Inhibition of Bmp signaling affects growth and differentiation in the anagen hair follicle. EMBO J. *19*, 6664–6674.

Kurose, K., Mori, O., Hachisuka, H., Shimizu, H., Owaribe, K., and Hashimoto, T. (2000). Cultured keratinocytes from plectin/HD1-deficient epidermolysis bullosa simplex showed altered ability of adhesion to the matrix. J. Dermatol. Sci. *24*, 184–189.

Kurzen, H., Moll, I., Moll, R., Schafer, S., Simics, E., Amagai, M., Wheelock, M.J., and Franke, W.W. (1998). Compositionally different desmosomes in the various compartments of the human hair follicle. Differentiation *63*, 295–304.

Lathrop, G.M., Lalouel, J.M., Julier, C., and Ott, J. (1984). Strategies for multilocus linkage analysis in humans. Proc. Natl. Acad. Sci. USA *81*, 3443–3446.

McGrath, J.A., McMillan, J.R., Shemanko, C.S., Runswick, S.K., Leigh, I.M., Lane, E.B., Garrod, D.R., and Eady, R.A. (1997). Mutations in the plakophilin 1 gene result in ectodermal dysplasia/skin fragility syndrome. Nat. Genet. *17*, 240–244.

McKoy, G., Protonotarios, N., Crosby, A., Tsatsopoulou, A., Anastasakis, A., Coonar, A., Norman, M., Baboonian, C., Jeffery, S., and McKenna, W.J. (2000). Identification of a deletion in plakoglobin in arrhythmogenic right ventricular cardiomyopathy with palmoplantar keratoderma and woolly hair (Naxos disease). Lancet *355*, 2119–2124.

McMillan, J.R., and Shimizu, H. (2001). Desmosomes: structure and function in normal and diseased epidermis. J. Dermatol. *28*, 291–298.

Mendelsohn, C., Batourina, E., Fung, S., Gilbert, T., and Dodd, J. (1999). Stromal cells mediate retinoid-dependent functions essential for renal development. Development *126*, 1139–1148.

Montagutelli, X., Hogan, M.E., Aubin, G., Lalouette, A., Guenet, J.L., King, L.E., Jr., and Sundberg, J.P. (1996). Lanceolate hair (lah): a recessive mouse mutation with alopecia and abnormal hair. J. Invest. Dermatol. *107*, 20–25.

Montagutelli, X., Lalouette, A., Boulouis, H.J., Guenet, J.L., and Sundberg, J.P. (1997). Vesicle formation and follicular root sheath separation in mice homozygous for deleterious alleles at the balding (bal) locus. J. Invest. Dermatol. *109*, 324–328.

Morris, R.J., and Potten, C.S. (1994). Slowly cycling (label-retaining) epidermal cells behave like clonogenic stem cells in vitro. Cell Prolif. *27*, 279–289.

Nguyen, V.T., Ndoye, A., Shultz, L.D., Pittelkow, M.R., and Grando, S.A. (2000). Antibodies against keratinocyte antigens other than desmogleins 1 and 3 can induce pemphigus vulgaris-like lesions. J. Clin. Invest. *106*, 1467–1479.

Norgett, E.E., Hatsell, S.J., Carvajal-Huerta, L., Cabezas, J.C., Common, J., Purkis, P.E., Whittock, N., Leigh, I.M., Stevens, H.P., and Kelsell, D.P. (2000). Recessive mutation in desmoplakin disrupts desmoplakin-intermediate filament interactions and causes dilated cardiomyopathy, woolly hair and keratoderma. Hum. Mol. Genet. *9*, 2761–2766.

Orwin, D.F. (1979). The cytology and cytochemistry of the wool follicle. Int. Rev. Cytol. *60*, 331–374.

Paine-Saunders, S., Viviano, B.L., Economides, A.N., and Saunders, S. (2002). Heparan sulfate proteoglycans retain Noggin at the cell surface: a potential mechanism for shaping bone morphogenetic protein gradients. J. Biol. Chem. *277*, 2089–2096.

Pulkkinen, L., Choi, Y.W., Simpson, A., Montagutelli, X., Sundberg, J., Uitto, J., and Mahoney, M.G. (2002). Loss of cell adhesion in Dsg3bal-Pas mice with homozygous deletion mutation (2079del14) in the desmoglein 3 gene. J. Invest. Dermatol. *119*, 1237–1243.

Pulkkinen, L., Choi, Y.W., Kljuic, A., Uitto, J., and Mahoney, M.G. (2003). Novel member of the mouse desmoglein family: Dsg1-β. Exp. Dermatol. *12*, 11–19.

Rikimaru, K., Moles, J.P., and Watt, F.M. (1997). Correlation between hyperproliferation and suprabasal integrin expression in human epidermis reconstituted in culture. Exp. Dermatol. *6*, 214–221.

Roth, S.I., and Helwig, E.B. (1964). The Cytology of the Dermal Papilla, the Bulb, and the Root Sheaths of the Mouse Hair. J. Ultrastruct. Mol. Struct. Res. *11*, 33–51.

Sambrook, J., Fritsch, E.F., and Maniatis, T. (1989). Molecular Cloning: A Laboratory Manual, 2nd Edition (Cold Spring Harbor, New York: Cold Spring Harbor Laboratory Press).

Sobel, E., and Lange, K. (1996). Descent graphs in pedigree analysis: applications to haplotyping, location scores, and marker-sharing statistics. Am. J. Hum. Genet. *58*, 1323–1337.

Sundberg, J.P., Boggess, D., Bascom, C., Limberg, B.J., Shultz, L.D., Sundberg, B.A., King L.E., Jr, and Montagutelli, X. (2000). Lanceolate hair-J (lahJ): a mouse model for human hair disorders. Exp Dermatol. *9*, 206–218.

Thompson, J.D., Plewniak, F., and Poch, O. (1999). A comprehensive comparison of multiple sequence alignment programs. Nucleic Acids Res. *27*, 2682–2690.

Tong, X., and Coulombe, P.A. (2003). Mouse models of alopecia: identifying structural genes that are baldly needed. Trends Mol. Med. *9*, 79–84.

Van Scott, E.J., Ekel, T.M., and Auerbach, R. (1963). Determinants of rate and kinetics of cell division in scalp hair. J. Invest. Dermatol. *4*, 269–273.

Accession Numbers

The final cDNA sequence of mouse *Dsg4* and human *DSG4* were deposited under GenBank accession number AY227349 and AY227350, respectively.